Seasonal monitoring and estimation of regional aerosol distribution over Po Valley, northern Italy, using high-resolution MAIAC product

Barbara Arvani[1], R. Bradley Pierce[2], Alexei I. Lyapustin[3], Yujie Wang[4], Grazia Ghermandi[1] and Sergio Teggi[1]

[1]{Dipartimento di Ingegneria Enzo Ferrari, Università di Modena e Reggio Emilia, via P. Vivarelli 10, 41125 Modena, Italy}

[2]{NOAA/NESDIS Advanced Satellite Products Branch, 1225 W. Dayton Street, Madison, WI 53706, USA}

[3]{NASA Goddard Space Flight Center, code 613, Greenbelt, Maryland 20771 USA}

[4]{University of Maryland, Baltimore County, 1000 Hilltop Circle, Baltimore, MD, USA}

Correspondence to: B. Arvani (barbara.arvani@unimore.it)

Abstract

In this work, the new 1-km-resolved Multi-Angle Implementation of Atmospheric Correction (MAIAC) algorithm is employed to characterize seasonal AOD-PM_{10} correlations over northern Italy. The accuracy of the new dataset is assessed versus the widely used Moderate Resolution Imaging Spectroradiometer (MODIS) Collection 5.1 Aerosol Optical Depth (AOD) data, retrieved at 0.55 μm with spatial resolution of 10 km (MYD04). We focused on evaluating the ability of these two products to characterize both temporal and spatial distributions of aerosols within urban and suburban areas. Ground PM_{10} measurements were obtained from 73 of the Italian Regional Agency for Environmental Protection (ARPA) monitoring stations, spread across northern Italy, for a three-year period from 2010 to 2012. The Po Valley area (northern Italy) was chosen as the study domain because of severe urban air pollution, resulting from the highest population and industrial manufacturing density in the country, being located in a valley where two surrounding mountain chains favor the stagnation of pollutants. We found that the global correlations between PM_{10} and AOD are $R^2 = 0.83$ and $R^2 = 0.44$ for MYD04_L2 and for MAIAC, respectively, suggesting for a greater sensitiveness of the high-resolution product to small-scale deviations. However, the introduction of Relative Humidity (RH) and

Planetary Boundary Layer (PBL) depth corrections gave a significant improvement to the PM – AOD correlation, which led to similar performance: $R^2 = 0.96$ for MODIS and $R^2 = 0.95$ for MAIAC. Furthermore, the introduction of the PBL information in the corrected AOD values was found to be crucial in order to capture the clear seasonal cycle shown by measured PM_{10} values. The study allowed us to define four seasonal linear correlations that estimate PM_{10} concentrations satisfactorily from the remotely sensed MAIAC AOD retrieval. Overall, the results show that the high resolution provided by MAIAC retrieval data is much more relevant than 10km MODIS data to characterize PM_{10} in this region of Italy which has a pretty limited geographical domain, but a broad variety of land usages and consequent particulate concentrations.

1 Introduction

Particulate matter (PM), also defined as atmospheric aerosol, is one of the major pollutants studied and monitored since it affects air quality in urban and rural areas worldwide. PM is the general term used to define a complex mixture of solid and liquid particles. These particles vary in size and composition, and remain suspended in the air for different periods of time. The sources of the atmospheric aerosols include both natural activity, such as fire, sea salt, volcanic eruptions and windblown dust, and anthropogenic activity, such as combustion, traffic and industrial emissions. PM with aerodynamic diameter of 10μm or less (PM_{10}) leads to serious human health effects. They can be inhaled into the respiratory system and so cause respiratory lung diseases and even premature death (Pope et al., 2004, Forastiere et al., 2005, Brunekreef and Forsberg, 2005). At local scale, urban pollution plays a significant role on issues related to health due to high urban population densities. Prior to the twentieth century, most urban air pollution problems arose from the burning of wood, cool and other raw materials without any emission controls. Such burning resulted in significant increases in health issues related to urban pollution (Jacobson, 2012).

The Po Valley, in the northern part of Italy, is the area with the most severe air pollution problems in the country and Europe as it is the largest industrial, trading and agricultural area with a high population density (Mélin and Zibordi, 2005, Bigi et al., 2012, Bigi and Ghermandi, 2014, Putaud et al., 2014). The pollution problems that affect the Po Valley are not only related to the presence of highly urbanized and industrial centers. In fact, the presence of the Alpine mountain chain at the North and West sides of the valley, and the Apennines to the South, act

as a barrier to winds blowing from Northern Europe and the Mediterranean, favoring stagnation conditions and accumulation of pollutants (Putaud et al., 2004, Mazzola et al., 2010, Putaud et al., 2010). Because of this, monitoring in this area requires data with high spatial resolution to better characterize the spatial variability of pollution within the Po Valley.

Due to health problems associated with urban air pollution, many environmental protection agencies have been developing capabilities for continuous monitoring and assessment of air pollution from ground-based stations and for improving sampling techniques. These ground-based measurements are necessary to guide studies of possible ways to reduce the air pollution problems. Yet, ground-based observations represent point measurements and do not have the necessary coverage to characterize the regional distribution of aerosols in the atmosphere. Moreover, the PM ground-based stations only provide information at the surface. The development of satellite remote sensing aerosol products since the launch of the Moderate resolution Imaging Spectroradiometer (MODIS) onboard the NASA Terra and Aqua satellites has permitted the exploration of new research techniques for monitoring global air quality (Gupta et al., 2006, Fishman et al., 2008). This alternative approach for air quality monitoring provides air quality data where the ground-based measurements are not available. The potential for using space-based sensors for the air quality monitoring was demonstrated using Aerosol Optical Depth (AOD) data in combination with the PM ground-based stations, as the literature suggest (Chu et al., 2003, Wang and Christopher, 2003). The use of MODIS aerosol products to investigate air pollution was demonstrated both in research fields (van Donkelaar et al., 2006, Gupta and Christopher, 2008b, Tian and Chen, 2010) and for operational applications (Al-Saadi et al., 2005). But, satellite AOD quantifies the presence of aerosols in an atmospheric column, while the surface PM mass concentration is needed for the assessment of air quality health impacts: it is not obvious what the relationship between these two quantities is for a particular region. Hoff and Christopher (2009) provide a detailed review of the literature on how satellite remote sensing provides an alternative way to monitor surface PM mass concentrations. As they point out, correlations between ground measurements and optical thickness are actively used and investigated.

In previous works, the Po Valley domain was studied, where the air quality monitoring from satellite measurements was applied (Di Nicolantonio et al., 2007, Di Nicolantonio et al., 2009, Barnaba et al., 2010). These studies pointed to the use of satellite remote sensing observations for monitoring the air pollution over industrialized and urban areas, such as the Po Valley.

However, their correlation is often not high enough for AOD retrievals to be operationally incorporated in air quality monitoring procedures. The MODIS standard aerosol product spatial resolution is appropriate for application on regional to global scale. However, its nominal resolution at nadir (10 km) may be too coarse to resolve urban scale processes. Therefore, alternative aerosol retrieval algorithms have been developed using the MODIS data in order to produce a finer high-spatial resolution product. The MODIS NASA research team recently released a new MODIS product: MODIS Collection 6, which includes a global aerosol product at nominal 3 km, in addition to the standard MYD04 at 10 km (Remer et al., 2013, Munchak et al., 2013, Livingston et al., 2014). Recently, the Multi-Angle Implementation of Atmospheric Correction (MAIAC) algorithm was developed for MODIS (Lyapustin et al., 2011a, Lyapustin et al., 2011b, Lyapustin et al., 2011c, Lyapustin et al., 2012). The MAIAC algorithm performs a simultaneous retrieval of surface Bidirectional Reflection Distribution Function (BRDF) and aerosol properties at a resolution of 1 km, and represents an interesting alternative for characterizing spatial variability of aerosol within polluted and industrial urban areas (Emili et al., 2011, Chudnovsky et al., 2013a, Chudnovsky et al., 2013b, Hu et al., 2014). Due to the availability of high-spatial resolution products, recently, a series of studies have demonstrated how the satellite remote sensing products can provide a potentially cost effective way to predict PM (PM_{10} and $PM_{2.5}$) concentrations by using AOD in areas where ground monitoring is either not available or too sparse (Chudnovsky et al., 2014, Hu et al., 2014a, Hu et al., 2014b, Kloog et al., 2014, Kloog et al., 2015, Just et al., 2015).

In the current study, we extend the preliminary analysis of Arvani et al. (2013b) by using the MAIAC 1 km resolution retrievals to analyze the relationship between PM_{10} mass concentration and remotely sensed AOD within the Po Valley, for an extended period of three years, from 2010 to 2012. We started with a direct comparison between both MYD04_L2 and MAIAC AOD retrievals and the surface PM_{10} measurements. Then, with the introduction of additional meteorological information, as the role of the planetary boundary layer and relative humidity, we analyzed the seasonal temporal and spatial variability of PM_{10} compared to AOD, for the same days and locations. Finally, starting from a monthly sweep of linear correlation coefficients, carried out on the 36 months where both datasets were available, we defined four unique correlations to estimate the PM_{10} concentrations on a seasonal level. The coefficients were obtained for both the coarse 10 km MYD04 and the finer high spatial resolution 1 km MAIAC satellite products.

2 Data and methods

2.1 Region of interest

The region of interest, Po Valley in northern Italy, shown in Fig. 1, covers an area of approximately 40° - 50° N and 5° - 15° E. In this paper, we considered three of its administrative regions, west to east: Piemonte, Lombardia and Emilia Romagna. Piemonte is characterized by major urban centers and is heavily industrialized. Most of the Italian Regional Agency for Environmental Protection (ARPA) network stations within the Piemonte region is located near the Alps. Lombardia is the most populated region, and it has the highest density of industrial sites. The Emilia Romagna region, similar to Piemonte, is characterized by major urban centers. Some of the ARPA sites within this region are located close to the Apennine mountain chain to the south, and near the coast of the Adriatic Sea to the east.

2.2 Ground-level mass concentration

Twenty-four hour averaged PM_{10} mass concentrations in μgm^{-3}, were obtained for 73 air quality monitoring ground-based stations within the ARPA network over a time span of 3 years, from 2010 to 2012: Piemonte (18 stations), Lombardia (19 stations), Emilia Romagna (36 stations). The spatial distribution of the ground-based stations almost uniformly covers most of the valley, as highlighted in Fig. 1. Each regional ARPA network has a unique set of measurements, carried out with different hardware and according to different daily averaging rules, thus leading to regionally different uncertainties. This non-uniformity may affect the correlations. In particular, in ARPA Piemonte PM_{10} is measured using a Beta Attenuation Monitor (BAM) with an accuracy of 2%. In ARPA Lombardia TEOM, TEOM-FDMS (Tapered Element Oscillating Micro-balance - Filter Dynamics Measurement System), or BAM are used, with an accuracy of $\pm 2.5\ \mu gm^{-3}$. In ARPA Emilia Romagna, PM_{10} data have been collected by the beta attenuator SWAM 5A RL by FAI Instruments with an uncertainty lower than ±10%. All information related to the ARPA's stations and instrumentation are available at the ARPA web sites of their respective regions, mentioned above. Yet all the instruments used are equivalent to the gravimetric technique, inserted within the framework of the EC Directive on ambient air quality and cleaner air for Europe (2008/50/EC).

2.3 Remotely sensed data

In the present work, we compare plain, standard MODIS Aqua Collection 5.1 (MYD04) aerosol product data with a first application of the high-resolution MAIAC algorithm over the Po valley. MYD04 data have a nominal spatial resolution of 10 km at nadir, which increases by roughly four-fold at the edges of the swath. The MODIS AOD algorithm uses multispectral observed radiance and pre-computed look-up tables to retrieve AOD over ocean and land (Remer et al., 2005, Remer et al., 2009). The recently developed MAIAC aerosol retrieval algorithm (Lyapustin et al., 2011a, Lyapustin et al., 2011b) employs MODIS Aqua Land retrieval data and is thus provided over the land only. AOD is retrieved at a finer spatial resolution (1 km), making simultaneous use of BRDF parameters. This is accomplished by using the time series of MODIS measurements and simultaneous processing of groups of pixels. The MAIAC algorithm guarantees that the number of measurements exceeds the number of unknowns, a necessary condition for solving an inverse problem without empirical assumptions, which are commonly used in current operational algorithms. The MAIAC time series approach also provides coverage at multiple (15) view angles for every surface grid cell, which is required for the BRDF retrievals from MODIS data. Moreover, MAIAC incorporates a Cloud Mask (CM) algorithm based on spatio-temporal analysis, which augments traditional pixel-level cloud detection techniques (Lyapustin et al., 2008). Fig. 2 shows three example days of MYD04 compared to MAIAC AOD retrieval, one day per each year of analysis (from 2010 to 2012). Since the study domain of the Po Valley has limited geographical extents, assessing 1 km MAIAC AOD retrievals which can achieve much greater detail than the standard MODIS product is extremely promising for future applications of the satellite measurements as part of predictive tools. The 10 km resolution of MODIS AOD does not allow local details of the AOD field to be detected. On the contrary, 1 km AOD retrievals allow areas of intense air pollution to be detected on the urban scale, such as Fig. 2 shows for June 5th, 2010 and March 16th, 2012. Furthermore, the high spatial resolution MAIAC retrieval often provides data where MODIS has reduced data coverage; for instance, the east coast of the Po Valley (marshland area), on April 19th, 2011. This is allowed by the time-series-based analysis and angle-based interpolation the MAIAC algorithm incorporates. A good review of this phenomenon is thoroughly explained in Emili et al., 2011, where five different days over the Alpine chain are considered and compared.

The MODIS Collection 5.1 retrieval has already been cloud filtered and is used without additional quality control. On the contrary, the new aerosol retrieval algorithm MAIAC includes masks of cloud and terrain, incorporated into the AOD Quality Assurance (QA) parameter definition. The MAIAC Cloud Mask (CM) and the Land-Water-Snow (LWS) mask fields have been considered during the MAIAC run in order to avoid pixels where clouds, water or snow are detected. As a matter of fact, one of the fundamental limitations of satellite data is the unavailability of air pollution observations both when clouds obstruct the satellite sensors field of view and over domains with high reflectivity surfaces such as urban areas or when snow and ice conditions predominate (Gupta and Christopher, 2008b, Emili et al., 2011). In Fig. 2, March 16th 2012, lack of AOD retrieval close to the important industrialized centers of Milan and Turin appears to be due to an intense pollution haze, which causes a total backscattering (gas and aerosol scattering) of the radiance to the sensor and seems to be misinterpreted as a cloud.

2.4 Meteorological data

The vertical span of the aerosol distribution defines the most relevant weighting parameter for the AOD datum. This was introduced by considering Planetary Boundary Layer (PBL) depth information. Relative Humidity (RH) was also introduced as a correction to dried PM_{10} mass concentration measurements. These parameters were obtained from 6 hourly analysis files from the NOAA National Center for Environmental Prediction (NCEP) Global Data Assimilation System (GDAS), downloaded from nomads.ncdc.noaa.gov, with a spatial grid resolution of 0.5°x0.5°. For each day, four analysis files are available, one per each synoptic hour (00, 06, 12 and 18 UTC). Therefore, 6 hourly meteorological files were interpolated on a time basis to the time of satellite overpass over the Po Valley domain. The PBL height is diagnostically determined and uses the bulk-Richardson (Troen and Mahrt, 1986) approach to iteratively estimate a PBL depth starting from the ground upward (Hong and Pan, 1996). Relative humidity in the GFS is computed according to the standard NCEP procedure:

- at T < -20 C, w.r.t. ice
- at T > 0 C, w.r.t. water
- -20 < T < 0, mix phased.

2.5 Spatial co-location of satellite data and ground measurements

The MODIS Collection 5.1 aerosol product, MAIAC retrievals and surface PM_{10} were co-located in space for the period from 2010 to 2012, for each ARPA station considered in the study domain. The spatial co-location of MODIS and MAIAC pixels with PM_{10} ground-based stations was accomplished using the average approach as suggested in Gupta et al. (2006) with a tolerance radius equal to 0.20° (about 20 - 25 km at the latitude of the Po Valley) for MYD04_L2 product, and 0.02° (about 2 - 2.5 km at the latitude of the Po Valley) for MAIAC, using the same scale factor as their spatial resolutions. To determine the coincidences, we considered that if there is at least one missing pixel within the tolerance area we set the mean AOD value equal to a missing data. This is a conservative approach since it automatically excludes all the retrievals in the neighborhood of pixels identified by the terrain and cloud masks within a fixed tolerance area. We find that the impact of neighboring missing values is less of an issue for the standard MODIS retrieval, possibly due to a more conservative cloud mask (Arvani et al., 2015).

2.6 Normalization of the AOD parameter

PM_{10} and AOD represent two different measurements of the atmospheric loading of aerosols. The PM_{10} is a dry mass concentration ($\mu g/m^3$), measured mostly ground level, at a specific geographic location. On the other hand, satellite AOD represents total column aerosol loading averaged over a specific spatial area (unitless) and it depends on the environmental conditions. As suggested by the literature, the PM - AOD correlation may be improved by considering meteorological information such as the role of the Relative Humidity (RH) (Li et al., 2005, Wang and Martin, 2007, Altaratz et al., 2013), or vertical distribution of aerosols (Gupta et al., 2006, Wang and Martin, 2007, Tsai et al., 2011). In this work, both the variations in the vertical distribution of aerosols and the role of the hygroscopic information are considered. For the first, the information on the Planetary Boundary Layer (PBL) depth is introduced. The use of PBL depth as parameter to improve the correlation between surface PM and satellite AOD measurements has utilized both as measurements (Boyouk et al., 2010, Barnaba et al., 2010, Tsai et al., 2011, Chu et al., 2013), and as model simulations (Gupta and Christopher, 2009, Emili et al., 2010), and is still widely used at present, such as in Chu et al., 2015, where vertical and horizontal distribution of aerosols over Baltimore - Washington Corridor are studied.

The Aerosol Optical Depth is defined as a vertical integral of aerosol extinction, from the surface to the top of the atmosphere (TOA):

$$AOD = \int_0^{TOA} \sigma_{0.55\,\mu m}^{ext}(z)dz \quad (1)$$

In Tsai et al., 2011, two types of aerosol vertical distributions are considered. The first assumes that the aerosols are well-mixed and confined in the PBL; the second one is characterized by two layers of aerosols, the first layer where the aerosols are well-mixed and a second layer with an exponential decay of aerosol extinction coefficient with height above the top of the first layer. The first type of vertical distribution is assumed in the current study. Mathematically this can be expressed as follows:

$$AOD^* = \sigma_{0.55\,\mu m}^{ZPBL} * ZPBL \quad (2)$$

where ZPBL represent the height of the PBL, schematically represented in Fig. 3. Under the hypothesis that most of the aerosols are confined and mixed homogeneously within the PBL, the values of AOD normalized by PBL height may be regarded as mean PBL extinction in km^{-1} ($\sigma_{0.55\,\mu m}^{ZPBL}$). It may be more representative of the surface PM_{10} concentration since variations in the depth of the PBL are accounted for. In this work, the normalization was applied both for MYD04 and MAIAC AOD retrievals.

In Fig. 4 panel (a) the monthly trend of PBL height is reported, for the entire period (2010-2012) and locations over the Po Valley domain. The box and whisker box graph was realized considering all the equal months in the period (3 years). The highest mean and median values were obtained during the summer, with the highest dispersion of data evaluated in terms of the different between the 10^{th} and 90^{th} percentiles, with a maximum for the month of July. On the contrary, the lowest mean and median values were obtained during the winter, with the lowest dispersion of data, with a minimum for the month of December. The statistical parameters obtained for the four seasons are shown in Fig. 5 panel (a). The highest mean and median values were obtained in summer (June, July, August), and the lowest in winter (December, January, February), which also presents the most limited dispersion features in contrary to the summer season. In spring (March, April, May) pretty high values were obtained, with a significant dispersion of data. In fall (September, October, November), instead, pretty low values were obtained, but slightly higher than the winter ones. It is important to mention that such seasonal changes were found under a complex and complete climatology study developed in Seidel et al. (2012) work. The paper states that, as a cross climatology overview, daytime values over

Europe occasionally reach 2 km in summer, and during spring and summer the PBL heights are higher than fall and winter. This confirms that the seasonal variations described above characterize the mixed layer values over the Po Valley domain.

2.7 Relative humidity correction

While the remotely sensed AOD value is the columnar aerosol abundance in ambient environment, the mass concentration of PM is a dry measure at a fixed RH. Therefore, as the literature suggests, introducing hygroscopic information on measured ground PM mass concentrations by means of a scaling function may be relevant.

Hence, we chose the relationship by Tsai et al. (2011), which was successfully applied to rather moist environments. This function expresses an aerosol growth factor *f(RH)* due to relative humidity as

$$f(RH) = \frac{1}{\left(1-\frac{RH}{100}\right)}, \quad (3)$$

where RH is the relative humidity value expressed in percentage.

In Fig. 4 panel (b) the monthly mean trend of RH for the Po Valley is reported. The highest mean and median values were seen during September, with a mean relative humidity of 35% and the highest dispersion of data evaluated in terms of the different between the 10^{th} and 90^{th} percentiles for the months of October and November leading to the formation of typical humid morning and occurrence of mild to heavy fog. The seasonal trend of relative humidity is shown in Fig. 5 panel (b). The highest mean and median values were obtained during the fall, and in summer. However, while dispersion is maximum during the fall, it is minimum in the summer. The lowest mean and median values were obtained during the winter.

In the section below, we consider the simple expression defined in (3) to test how the RH affects the PM_{10} – AOD correlation, AOD being normalized by PBL depth.

3 Results and discussion

3.1 PM_{10} vs. AOD correlation: binned scatter plot analysis

First of all, a direct comparison between daily PM_{10} mass concentrations and remotely sensed AOD values with no meteorological corrections was done. A non-corrected linear correlation

was obtained from both MYD04 and MAIAC, at all ground stations and for the whole 2010 to 2012 period.

Because of the evidently large spread of AOD and PM values (not reported in this paper, but shown in Arvani et al., 2013a for a limited period of time and domain of analysis), and not promising values of R^2 (see Table 1), we divided the AOD into 20 bins of 0.05 intervals for the range [0-1], and we compared them with the mean PM_{10} within each bin. So, the final PM-AOD correlation value is determined by using the average value of PM in each AOD bin. This set of twenty points is reported on the scatter plot as black dots in Fig. 6, panels (a). The solid red line shows the linear regression line for these two data sets. White dots refer to median values of AOD at fixed value of PM_{10}. Gray symbols represent the 25^{th} and 75^{th} percentile (first and third quartiles) respectively in PM_{10} for a particular AOD bin. *N*, on the top of each plot, represents the number of coincidence calculated from the full scatter plots, before binning, where by coincidence we mean a (station, date) case where both PM measurement and the AOD value are available. This simple statistical approach gives a robust estimate of the linear regression between the PM_{10} and satellite data (Gupta et al., 2006). Using this regression relation, obtained from the bin-averaged PM_{10} and AOD correlation, surface PM_{10} mass concentration can be quantified when the remotely sensed AOD is available and an estimate of the air quality index could be obtained. The correlation between bin-averaged AOD and PM_{10} concentration is highest for MYD04, with $R^2 = 0.83$. The higher resolution MAIAC retrieval algorithm has a significantly lower R^2 of 0.44. Looking at the result in Fig. 6 lower panels (a) this worst result may be due to the last bins, especially the last two ones that have values of mean, median and 75^{th} percentile completely out of range. A possible explanation of this would be correlated to the fact that we are looking to maximum edge of the possible values of AOD, therefore fewer values available for solid statistics. In agreement of this, both MYD04 and MAIAC correlation show a strange behavior for the last six bins, for the range [0.8-1].

As mentioned in the previous subsection, the PM_{10} – AOD correlation is not enough to estimate a mass concentration value from a remotely sensed measured. Therefore, the introduction of meteorological variables is necessary. Firstly, we introduced the PBL depth values, for the same period and locations of analysis. This leaded to consider the AOD/ZPBL vs. PM_{10} correlation, and we used the same procedure describe above. The results are summarized in Fig. 6, panels (b), for both MYD04_L2 and MAIAC retrievals. They show a significant improvements after the normalization, with an R^2 of 0.96 and 0.95 for MYD04_L2 and MAIAC, respectively. This

indicates that the introduction of well-mixed PBL information is mandatory for both remotely sensed measurements. Secondly, we introduced the RH correction on the mass concentration measurements. However, it did not produce improvements in the correlations, as reported in Fig. 6 panels (c).

This analysis suggested that the introduction of the hygroscopic factor on the PM mass concentration measurements seems produce a much less significant improvement in the PM – AOD correlation, and could hence be discarded for the current study, while the introduction of vertical distribution information cannot be avoided as it leads to a huge improvement.

3.2 Temporal trends of AOD and PM_{10} mass concentration

As second step of our study, we introduced time-series analysis to quantitatively examine the temporal trends of PM_{10} levels, as well as their AOD correlations.

In Fig. 7 upper panels, the monthly trend of the PM_{10} (a), the MODIS (b) and MAIAC (c) AOD are reported respectively, for the entire period (2010-2012) and locations over the Po Valley. PM_{10} and AOD monthly trends have opposite behavior for both retrievals. The PM_{10} monthly mean trend over a year is characterized by low mean and median values as well as limited dispersion during the summer months, and high mean and median values - with large dispersion - during the winter period. This is summarized by the corresponding seasonal statistics reported in Fig. 8 upper panel (a), which have been derived from the same data set for all locations and dates. During the spring and fall seasons, intermediate values smoothly follow the summer vs. winter behavior, the fall values being slightly higher than the spring ones.

On the other hand, the AOD monthly mean trends of Fig. 7, upper panels (b) and (c), for MYD04_L2 and MAIAC products, respectively, are characterized by high mean and median values with significant dispersion during the spring/summer period and low mean and median values with limited dispersion during the winter. Both retrievals show similar monthly trends, as also enforced by the seasonal statistics of Fig. 8 upper panels (b) and (c). The fact that seasonal statistics for both retrieval methods tend to converge to the same values suggests that MAIAC produces a reliable higher-resolution prediction, which fits the same averaged data as the coarser product. Seasonal high values of PM during the fall and winter can be partly related to the meteorological conditions that characterize the Po Valley. During these periods, in fact, events of strong temperature inversion, which favor the buildup of near-ground pollutants and lead to the formation of fog events, are frequent. When the pollutants are trapped within the

stable layer, they may stay with a residence time of the order of hours. Furthermore, intense human activities which characterize the area, with the largest presence of agriculture and industry levels of activities in Italy (Fuzzi et al., 1992, Di Nicolantonio et al., 2009, Mazzola et al., 2010), should also be regarded as responsible for this phenomenon. As far as the AOD trend is concerned, instead, high values of AOD (detected both by MODIS and MAIAC monthly mean trends) during the spring/summer period appear to be correlated in part to meteorological factors, like desert dust intrusions from northern Africa, transport of fire particles at the low latitude, and anthropogenic factors, like a long-range transport of aerosol produced by human activities from Central Europe (Mazzola et al., 2010). Yet, the limited dispersion of data recorded during the fall/winter period, which has a minimum in December, is correlated to often prohibitive conditions for the satellite to remotely sense the columnar abundance over the domain, due to intense and frequent formation of a layer of clouds, presence of snow or intense haze over the urban areas with high reflectivity (Gupta and Christopher, 2008a). In Table 2 the total number of dataset points, both for PM_{10} and AOD measurements, are reported. Considering all 73 locations and the whole 2010-2012 period (1096 days), the largest possible dataset would contain 80.008 measurements. While PM_{10} measurements are available for most days and locations (no data being provided only when instrumentation issues at the ground-based stations happened), the remotely sensed AOD values are only available at the 32% and 28% of the cases, for MYD04_L2 and MAIAC respectively.

In the lower row of Figure 7, panels (a), (b) and (c), instead, the monthly trend of PM_{10} mass concentration is corrected by the RH function of Eqn. (3), and the MODIS and MAIAC AOD values are both normalized by the PBL depth. In agreement to what verified in Section 3.1, the introduction of the hygroscopic factor, may not produce a significant alteration, but it appears to noticeably reduce data dispersion during the winter season. The seasonal statistics are again shown in Fig. 8, lower panel (a) confirm what observed above. On the other hand, the normalization of AOD by PBL depth produces significant changes in both the MODIS and MAIAC AOD trends. AOD/ZPBL monthly trends are now characterized by an opposite behavior than non-normalized AOD: low mean and median values, with limited dispersion, are seen during the summer months, and high mean and median values during the winter, with more intense dispersion. Seasonal statistics for AOD/ZPBL in Fig. 8 lower panels (b) and (c), for both retrievals, now show trends clearly mimic the behavior of RH-corrected measured PM_{10}. This significant improvement on the AOD side is caused by the PBL height – whose

monthly mean trend is presented in Section 2.6 - which reaches the highest value during the spring/summer period.

3.3 Spatial trends of AOD and PM_{10} mass concentration

Fig. 9 upper panel (a) shows the mean spatial distribution of ground PM_{10} measurements from ARPA sites, compared with the mean spatial distribution of AOD values for both MODIS and MAIAC retrievals (upper panels (b) and (c)), across all years (2010-2012) and locations. MAIAC AOD seems to replicate the major spatial pattern of ground measurements of PM_{10} in the east side of the valley and near the coast. On the other hand, high values of PM_{10} measured close the major urban and industrialized sites of Milan and Turin is not well detected by both the non-corrected AOD retrievals. The second row of Fig. 9 compares instead global time averages of relative-humidity-corrected measured PM_{10} measurements – panel (a) – with PBL-normalized AOD for both MODIS and MAIAC (panels (b) and (c)), at each monitoring site. PBL information has a significant impact on MODIS retrievals in the southeast of the valley and on the southern edge (near-mountain stations), where normalized AOD have significantly smaller values. MAIAC AOD spatial distribution is instead less affected in those regions – fewer coincidences being invalid because of cloud cover or snow-related reflectance (different cloud mask). This led MAIAC to better replicating the major spatial pattern shown by PM_{10} ground measurements, also near the major northwestern urban and industrialized sites, where a consistent increase of normalized AOD's was seen versus the non-normalized ones. The RH correction impact on the PM_{10} measurements was of increasing the PM values anywhere. The effect was however particularly evident at the sites that exhibited the largest PM_{10} averages, i.e., the urban and industrialized sites of Milan and Turin.

The seasonal spatial trends are reported in Fig. 10. The largest impact of a correction is seen for AOD normalization during the winter. Here (lower panels (b) and (c)), both MODIS and MAIAC retrievals show significantly higher values when PBL-normalized, for all sites in the valley. RH correction is again less relevant. However, it has a positive effect across all seaons in terms of better "distinguishing", or increasing the local gradients of PM_{10}, between the urban versus the mountain areas. While before the correction PM_{10} presents an almost flat spatial trend on the valley, the RH-corrected spatial trend provides much more comparable data to the PBL-normalized AOD values of lower panel (c). Again, MAIAC provides a better comparison with measured data than MODIS, where the spatial results are much more scattered. Looking

at the other three seasons (Spring, Summer and Fall), they have lower values than in winter because of the larger PBL heights. However, the improvement in local gradient distribution is still evident, even if up to a smaller extent.

The seasonal spatial trends analysis presented in this section suggests that normalized AOD spatial trends present a comparable pattern to the PM_{10} measured one for MAIAC, while the MODIS spatial trend, as an effect of its much coarser spatial resolution, suffers from more data dispersion especially during the winter season where the retrievals are fewer and less reliable.

3.4 Estimation of PM_{10} using the coarse MYD04 and the fine MAIAC products

As last step of our study in this paper, we introduced linear relationship to estimate PM_{10} concentrations, using both the coarse 10 km MYD04 and the high-resolution 1 km MAIAC products.

We started to examine the linear correlation coefficients monthly trends, reported in Fig. 11, for both the AOD retrievals (MODIS 10 km in upper and lower panels (a) and MAIAC 1 km in upper and lower panels (b)), and for entire period of analysis. In order to assess the effect of the AOD correction, linear correlation coefficients were obtained by correlating monthly PM_{10} measurements with MYD04 and MAIAC, both with (Fig. 11, second row) and without (first row) PBL depth normalization. The intercepts, which provide a 'ground' or 'noise' PM value to be applied when AOD is zero, are not influenced by the correction of meteorological variables. Slope trends show instead much different behaviors. The annual trend tends to disappear into a flat line when AOD is PBL-normalized; for both retrievals, the slopes are similar, and fluctuate around the global average of 17.9 for MODIS and 21.7 for MAIAC.

The seasonal coefficients were directly obtained from this analysis, and are listed in Table 3. For each season, a slope and an intercept value were found as the means of their corresponding monthly mean values. For the PM_{10} – AOD correlation type, MAIAC shows a tendency towards lower intercepts than MYD04, and correspondingly higher slopes; both retrievals showing similar correlation coefficients, R^2. For the normalized PM_{10} – AOD/ZPBL relationship, while the intercepts remain lower for MAIAC, the slopes now show similar results as the MODIS ones. This suggests that the PBL normalization brings a more stable, closer-to-linear relationship between the ground measurement and the satellite datum for both retrievals. Therefore, we used the four intercepts and slopes for the normalized AOD datum to define four corresponding seasonal correlations (4a – 4b – 4c – 4d):

$$Y_{MAM} = m_{MAM} * X + q_{MAM} \quad (4a)$$

$$Y_{JJA} = m_{JJA} * X + q_{JJA} \quad (4b)$$

$$Y_{SON} = m_{SON} * X + q_{SON} \quad (4c)$$

$$Y_{DJF} = m_{DJF} * X + q_{DJF} \quad (4d)$$

where Y represents estimated PM_{10} map concentrations and X the corresponding map of normalized AOD/ZPBL values for both the coarse MODIS AOD product and the finer high-resolution MAIAC. Fig. 12 and Fig. 13 show twelve one-day examples of estimated (map) and measured (dots) PM_{10} concentrations, one for each month. The estimate was made using MYD04 at 10 km spatial resolution (Fig. 12) and MAIAC AOD retrieval at 1 km spatial resolution (Fig. 13), respectively. The available PM_{10} in-situ measurements are displayed on top of the PM_{10} estimated map of concentrations, with the same concentration scale. The patterns of PM_{10} concentrations predicted by both MYD04 and MAIAC retrievals are similar in spring and summer, when the pollutant levels remain moderate. During the fall and winter seasons, when the pollutant levels reach the highest values, MAIAC is able to better capture the major spatial gradients shown by measured PM_{10}. The coarse 10 km MYD04 product does not allow the PM_{10} concentrations to be well detected on a local scale, and it is also affected by reduced data coverage. The dates of November 16th, December 5th and January 26th, show regions where it is possible to estimate the PM10 concentrations using MAIAC, but where MODIS data at 10 km is not available. This suggest MAIAC's better potential to serve PM_{10} studies in the Po Valley, which is characterized by high cloud cover values for many days during a year, especially during the fall and winter seasons where PM values are maximum.

To assess the goodness of fit of the estimated values, two statistical indicators such as the Root Mean Square Error (RMSE) and the coefficient of determination (R^2) were calculated between the predicted PM_{10} concentrations and the observations. The seasonal results of the used statistical indicators are listed in Table 4. The RMSE ranges from 6.91 in summer to 8.58 $\mu g/m^3$ in spring for MYD04, and from 6.63 in summer to 15.10 $\mu g/m^3$ in winter for MAIAC. Overall, the results indicate a good fit between predicted PM_{10} concentration values and the observations. In particular, looking at MAIAC RMSE values, the high-spatial resolution product provides slightly better RMSE values on spring and summer, and worst for the fall and winter seasons. For instance, in winter MAIAC has a RMSE which is 50% higher than the MODIS result. For both the retrievals, the lowest error was obtained in summer, where the

pollutant concentrations reach the lowest levels and the meteorological condition of cloudless permits the highest number of available remotely sensed data. After the normalization by the ZPBL on both MYD04 and MAIAC AOD retrievals, the RMSE range changes as from 5.33 in winter to 8.33 $\mu g/m^3$ in spring and from 6.45 in summer to 11.45 $\mu g/m^3$ in winter, respectively. The introduction of the meteorological variable on the AOD retrieval, not only increments the PM – AOD correlation and improves the temporal and spatial trends, but also reduces the existing error between predicted and measured PM_{10} concentrations. This is true for both retrievals. Also in this case, MAIAC is slightly better in spring and summer, but worse in fall and winter where the AOD retrieval rate is less. The discrepancy between the winter RMSE for MODIS and the winter RMSE for MAIAC is still around 47%, also after the normalization. While MAIAC obtained the lowest error in summer, MODIS did it in winter, apparently in contradiction to what stated before. Regarding the coefficient of determination, the results show that R^2 is relatively low – ranging from 0.46 down to 0.04 for MODIS, and from 0.26 to 0.16 for MAIAC. Both retrievals show that the highest R^2 was obtained in the summer, with a maximum number of AOD retrievals, whereas the lowest was obtained in winter, with a minimum number of AOD retrievals. On average, MAIAC show slightly worse results in spring and summer. Yet, an improvement was obtained for the fall and winter seasons. While the normalization by the ZPBL variable seems to slightly improve the R^2 values for MODIS retrievals (except in winter), on average in MAIAC the statistical indicator become worse, in each season.

4 Concluding Remarks

Until recently, the MODIS satellite AOD data product, with 10 km resolution, was the main source of global satellite aerosol data used by the air quality community. The new MAIAC AOD product, at 1 km resolution, provides a significantly higher resolution that may be more appropriate for urban air quality studies. This paper analyzed the effect of spatial resolution on the correlation between remotely sensed AOD and ground-based PM_{10} concentration measurements and the estimation of the PM_{10} concentrations from the high-spatial resolution at 1 km product over the Po valley domain, in northern Italy. Three years, from 2010 to 2012, of MODIS Aqua and MAIAC AOD retrievals were used. The study also focused on seasonal trends in the Po valley, and their effect on the accuracy of the retrievals.

Based on this study, the following conclusions were drawn:

1. A direct comparison between coarse MYD04_L2 10 km AOD and high-resolution MAIAC 1 km AOD for all collocated PM vs. AOD pairs for the same period of analysis and sites showed that both retrievals have pretty low correlation coefficients, if PM-AOD points are not binned into a number of AOD 'classes';

2. The link between surface measurements and AOD data alone not suitable for quantitative analysis. The normalization of the optical parameter AOD by the PBL depth significantly improves the R^2, and is also able to capture seasonal changes in the PBL height over the Po Valley. Similar global correlation coefficients, $R^2 = 0.96$ and $R^2 = 0.95$, were obtained for standard MODIS and MAIAC retrievals, respectively, when considering all the period and locations.

3. The seasonal temporal analysis showed opposite trends for non-normalized monthly mean AOD versus the PM_{10} mass concentrations. This strengthened the need to always apply the mixing layer correction in order to achieve a suitable AOD monthly mean trend, resulting proportional with the PM one.

4. The study of how the relationship of AOD and dehumidified PM at surface is affected by relative humidity (RH) showed that seasonal changes in AOD are more prominent compared to seasonal changes in PM_{10} mass concentrations, and that the RH correction on the PM mass concentration measurement did not significantly improve the PM – AOD correlation in this area, which is affected by a rather homogeneous relative humidity concentration all year long (Fig. 4 b).

5. The seasonal spatial analysis showed acceptable agreement between the MAIAC AOD retrieval after the PBL normalization and the PM_{10} measurements after the RH correction. This agreement is even better during the winter season, when the pollutant values are maximum, especially close to the major urban and industrialized sites.

6. The results obtained from the linearization procedure to estimate the PM_{10} concentrations showed that – if averaged over the whole domain – the MAIAC predicted PM_{10} concentrations at 1 km resolution are comparable with MODIS predicted PM_{10} concentrations at 10 km resolution. However, local values, relevant in a limited geographical domain such as the Po Valley, are substantially better when using the high spatial resolution MAIAC AOD product than MODIS, as more spatial details near the major

urban and industrialized areas in the domain are captured both by the satellite retrieval and by its seasonal PM_{10} estimation function.

Therefore, the study suggested that MAIAC has a good potential to provide data for PM_{10} concentration predictions and so it may be later be used to serve PM_{10} health effects studies in a narrow, populated, industrialized and urbanized domain, like the Po Valley in Italy.

In future studies, we will focus on two aspects. First, we will investigate further extensions of the satellite-retrieved AOD and PM_{10} relationships, such as by dividing the entire domain into areas to study the effects of different levels of urbanization on surface brightness and thus quality of the aerosol retrieval (cf. Lyapustin et al., 2011b). Second, the use of higher resolution PBL estimates over Italy (Kukkonen et al., 2012, Baldauf et al., 2011, Barthlott et al., 2010) will be used to explore the relationship for each administrative district over Po valley separately. The aim is to understand if the use of finer PBL depth and satellite – retrieved AOD (MAIAC) helps to better characterize the spatial variability of aerosol pollution within the Po Valley.

Acknowledgements

This research has been funded by the Italian Ministero dell'Istruzione, dell' Università e della Ricerca (Project PRIN2010-11, 2010WLNFY2). Authors are thankful to Italian agencies ARPA Emilia-Romagna, ARPA Lombardia, ARPA Piemonte and ARPA Veneto for providing ground PM_{10} data. The views, opinions, and findings contained in this report are those of the author(s) and should not be construed as an official National Oceanic and Atmospheric Administration or U.S. Government position, policy, or decision.

References

Al-Saadi, J., Szykman, J., Pierce, R. B., Kittaka, C., Neil, D.,Chu, D. A., Remer, L., Gumley, L., Prins, E., Weinstock, L., MacDonald, C., Wayland, R., Dimmick, F. and Fishman, J.: Improving National Air Quality Forecasts with Satellite Aerosol Observations, Bull. Amer. Meteor. Soc, 86, 1249–1261, BAMS-86-9-1249, 2005.

Altaratz, O., Bar-Or, R. Z., Wollner, U., & Koren, I. (2013). Relative humidity and its effect on aerosol optical depth in the vicinity of convective clouds. *Environmental Research Letters*, *8*(3), 034025, doi:10.1088/1748-9326/8/3/034025

Arvani, B., Pierce, R. B., Teggi, S., Bigi, A., & Ghermandi, G. (2013a). Implementation of IMAPP/IDEA-I over the Po Valley region, northern Italy, for air quality monitoring and forecasting. Proc. Cest.

Arvani, B., Pierce, R. B., Lyapustin, A. I., Wang, Y., Teggi, S., & Ghermandi, G. (2013b). Application of MAIAC high spatial resolution aerosol retrievals over Po Valley (Italy). Proc. SPIE 8890, Remote Sensing of Clouds and the Atmosphere XVIII; and Optics in Atmospheric Propagation and Adaptive Systems XVI, 88900P (17 October 2013), 8890-26, doi: 10.1117/12.2029297.

Arvani, B., Pierce, R. B., Lyapustin, A. I., Wang, Y., Ghermandi, G., & Teggi, S. (2015). High spatial resolution aerosol retrievals used for daily particulate matter monitoring over Po valley, northern Italy. Atmospheric Chemistry and Physics Discussions, 15(1), 123-155.

Baldauf, M., Seifert, A., Förstner, J., Majewski, D., Raschendorfer, M. and Reinhardt, T.: Operational Convective-Scale Numerical Weather Prediction with the COSMO Model: Description and Sensitivities, Monthly Weather Review, 139, 3887–3905, doi: 10.1175/MWR-**D**-10- 05013.1, 2011.

Barnaba F., Putaud, J.P.,Gruening C., dell'Acqua A., Dos Santos S., 2010. Annual cycle in collocated in situ, total-column, and height-resolved aerosol observations in the Po Valley (Italy): implications for ground-level particulate matter mass concentration estimation from remote sensing, J. Geophys. Res., 115, D19209, doi:10.1029/2009JD013002.

Barthlott, C., Schipper, J. W., Kalthoff, N., Adler, B., Kottmeier, C., Blyth, A. and Mobbs, S.: Model representation of boundary-layer convergence triggering deep convection over complex terrain: A case study from COPS, Atmospheric Research, 95, 172– 185, doi:10.1016/j.atmosres.2009.09.010, 2010.

Bigi, A. and Ghermandi, G. and Harrison, R. M.: Analysis of the air pollution climate at a background site in the Po valley, Journal of Environmental Monitoring, 14, 552-563, doi: 10.1039/C1EM10728C, 2012.

Bigi, A., & Ghermandi, G. (2014). Long-term trend and variability of atmospheric PM10 concentration in the Po Valley. *Atmospheric Chemistry and Physics*, *14*(10), 4895-4907, doi:10.5194/acp-14-4895-2014.

Boyouk, N., J. F. Léon, H. Delbarre, T. Podvin, and C. Deroo, 2010. Impact of themixing boundary layer on the relationship between PM2.5 and aerosol optical thickness, Atmos. Environ., 44, 271-277, doi:10.1016/j.atmosenv.2009.06.053.

Brunekreef, B. and Forsberg, B.: Epidemiological evidence of effects of coarse airborne particles on health, European Respiratory Journal, 26, 309–318, 2005.

Chu, D. A.,Kaufman, Y. J., Ichoku, C., Remer, L. A., Tanra, D. and Holben, B. N: Validation of MODIS aerosol optical depth retrieval over land, Geophysical Research Letters, 29, MOD2–1–MOD2–4, 2002.

Chu, D. A., Kaufman, Y. J., Zibordi, G., Chern, J. D., Mao, J., Li, C., and Holben, B. N.: Global monitoring of air pollution over land from the Earth Observing System- Terra Moderate Resolution Imaging Spectroradiometer (MODIS), Journal of Geophysical Research: Atmospheres, 108, NO. D21, 4661, doi: 10.1029/2002JD003179, 2003.

Chu, D. A., Tsai, T. C., Chen, J. P., Chang, S. C., Jeng, Y. J., Chiang, W. L., & Lin, N. H. (2013). Interpreting aerosol lidar profiles to better estimate surface PM 2.5 for columnar AOD measurements. *Atmospheric Environment*, *79*, 172-187, doi:10.1016/j.atmosenv.2013.06.03

Chu, D. A., Ferrare, R., Szykman, J., Lewis, J., Scarino, A., Hains, J., Burton, S., Chen, G., Tsai, T., Hostetler, C., Hair, J., Holben, B., Crawford, J., (2015). Regional characteristics of the relationship between columnar AOD and surface PM 2.5: Application of lidar aerosol extinction profiles over Baltimore–Washington Corridor during DISCOVER-AQ. *Atmospheric Environment*, *101*, 338-349, doi:10.1016/j.atmosenv.2014.11.034.

Chudnovsky, A., Tang, C., Lyapustin, A., Wang, Y., Schwartz, J., and Koutrakis, P.: A critical assessment of high-resolution aerosol optical depth retrievals for fine particulate matter predictions, Atmospheric Chemistry and Physics, 13, 10 907–10 917, 2013a.

Chudnovsky, A. A., Kostinski, A., Lyapustin, A., and Koutrakis, P.: Spatial scales of pollution from variable resolution satellite imaging, Environmental Pollution, 172, 131 – 138, 2013b.

Chudnovsky, A. A., Koutrakis, P., Kloog, I., Melly, S., Nordio, F., Lyapustin, A., ... & Schwartz, J. (2014). Fine particulate matter predictions using high resolution Aerosol Optical Depth (AOD) retrievals. Atmospheric Environment, 89, 189-198.

Di Nicolantonio, W., Cacciari, A., Bolzacchini, F., Ferrero, L., Volta, M., & Pisoni, E. (2007). MODIS aerosol optical properties over North Italy for estimating surface-level PM2. 5. In *Proceedings of Envisat Symposium* (pp. 3-27).

Di Nicolantonio, W., Cacciari, A., & Tomasi, C. (2009). Particulate matter at surface: Northern Italy monitoring based on satellite remote sensing, meteorological fields, and in-situ samplings. *Selected Topics in Applied Earth Observations and Remote Sensing, IEEE Journal of, 2*(4), 284-292.

"Directive 2008/50/EC of the European Parliament and of the Council of 21 May 2008 on "Ambient air quality and cleaner air for Europe"," *Official J.*, vol. L152, pp. 1–44, Nov. 6, 2008.

Emili, E., Popp, C., Petitta, M., Riffler, M., Wunderle, S., & Zebisch, M. (2010). PM 10 remote sensing from geostationary SEVIRI and polar-orbiting MODIS sensors over the complex terrain of the European Alpine region. *Remote sensing of environment, 114*(11), 2485-2499.

Emili, E., Lyapustin, A., Wang, Y., Popp, C., Korkin, S., Zebisch, M., Wunderle, S., and Petitta, M.: High spatial resolution aerosol retrieval with MAIAC: Application to mountain regions, Journal of Geophysical Research: Atmospheres, 116, D23211, doi: 10.1029/2011JD016297, 2011.

Fishman, J., Bowman, K. W., Burrows, J. P., Richter, A., Chance, 710 K. V., Edwards, D. P., Martin, R. V., Morris, G. A., Pierce, R. B., Ziemke, J. R., Schaack, T. K., Thompson, A. M.: Remote sensing of tropospheric pollution from space, Bulletin of the American Meteorological Society, 89, 805–822, 2008.

Forastiere, F. , Stafoggia, M. , Picciotto, S. , Bellander, T. , D'Ippoliti, D. , Lanki, T. , von Klot, S. , Nyberg, F. , Paatero, P. , Peters, A. , Pekkanen, J., Sunyer, J. and Perucci, C. A.: A Case-Crossover Analysis of Out-of-Hospital Coronary Deaths and Air Pollution in Rome, Italy, American journal of respiratory and critical care medicine, 172, 1549–1555, 2005.

Fuzzi, S., Facchini, M. C., Orsi, G., Lind, J. A., Wobrock, W., Kessel, M., ... & Georgii, H. W. (1992). The Po valley fog experiment 1989. Tellus B, 44(5), 448-468.

Gupta, P., Christopher, S. A., Wang, J., Gehrig, R., Lee, Y., and Kumar, N.: Satellite remote sensing of particulate matter and air quality assessment over global cities, Atmospheric Environment, 40, 5880 – 5892, 2006

Gupta, P., & Christopher, S. A. (2008). An evaluation of Terra-MODIS sampling for monthly and annual particulate matter air quality assessment over the Southeastern United States. *Atmospheric Environment*, *42*(26), 6465-6471, 2008a.

Gupta, P. and Christopher, S. A.: Seven year particulate matter air quality assessment from surface and satellite measurements, Atmospheric Chemistry and Physics, 8, 3311–3324, 2008b.

Gupta, P., and S. A. Christopher (2009), Particulate matter air quality assessment using integrated surface, satellite, and meteorological products: Multiple regression approach, J. Geophys. Res., 114, D14205, doi:10.1029/2008JD011496.

Hänel, G., 1976. The properties of atmospheric aerosol particles as functions of the relative humidity at thermodynamic equilibrium with surrounding moist air. Adv. Geophys. 19, 73e188.

Hoff, R. M. and Christopher, S. A.: Remote sensing of particulate pollution from space: have we reached the promised land?, Journal of the Air & Waste Management Association, 59, 645–675, 2009.

Holben, B., Eck, T., Slutsker, I., Tanré, D., Buis, J., Setzer, A., Vermote, E., Reagan, J., Kaufman, Y., Nakajima, T., Lavenu, F., Jankowiak, I., and Smirnov, A.: AERONET - A Federated Instrument Network and Data Archive for Aerosol Characterization, Remote Sensing of Environment, 66, 1 – 16, 1998.

Hong, S.-Y. and H.-L. Pan, 1996: Nonlocal boundary layer vertical diffusion in a medium-range forecast model. Mon. Wea. Rev., 124, 2322-2339

Hu, X., Waller, L. A., Lyapustin, A., Wang, Y., Al-Hamdan, M. Z., Crosson, W. L., Estes Jr, M. G., Estes, S. M., Quattrochi, D. A., Puttaswamy, S. J., Liu, Y.: Estimating ground-level $PM_{2.5}$ concentrations in the Southeastern United States using MAIAC AOD retrievals and a two-stage model, Remote Sensing of Environment, 140, 220–232, 2014a.

Hu, X., Waller, L. A., Lyapustin, A., Wang, Y., & Liu, Y. (2014b). 10-year spatial and temporal trends of PM 2.5 concentrations in the southeastern US estimated using high-resolution satellite data. Atmospheric Chemistry and Physics, 14(12), 6301-6314.

Jacobson, M. Z.: Air pollution and global warming: history, science, and solutions, Cambridge University Press, 2012.

Just, A. C., Wright, R. O., Schwartz, J., Coull, B. A., Baccarelli, A. A., Tellez-Rojo, M. M., ... & Kloog, I. (2015). Using high-resolution satellite aerosol optical depth to estimate daily PM2.

5 geographical distribution in Mexico City. Environmental science & technology, 49(14), 8576-8584.

Kloog, I., Chudnovsky, A. A., Just, A. C., Nordio, F., Koutrakis, P., Coull, B. A., ... & Schwartz, J. (2014). A new hybrid spatio-temporal model for estimating daily multi-year PM 2.5 concentrations across northeastern USA using high resolution aerosol optical depth data. Atmospheric Environment, 95, 581-590.

Kloog, I., Sorek-Hamer, M., Lyapustin, A., Coull, B., Wang, Y., Just, A. C., ... & Broday, D. M. (2015). Estimating daily PM 2.5 and PM 10 across the complex geo-climate region of Israel using MAIAC satellite-based AOD data. Atmospheric Environment.

Kuehn, R. E., Personal Communication, 2013.

Kukkonen, J., Olsson, T., Schultz, D. M., Baklanov, A., Klein, T., Miranda, A. I., Monteiro, A., Hirtl, M., Tarvainen, V., Boy, M., Peuch, V.-H., Poupkou, A., Kioutsioukis, I., Finardi, S., Sofiev, 760 M., Sokhi, R., Lehtinen, K. E. J., Karatzas, K., San Jose´, R., Astitha, M., Kallos, G., Schaap, M., Reimer, E., Jakobs, H., and Eben, K.: A review of operational, regional-scale, chemical weather forecasting models in Europe, Atmospheric Chemistry and Physics, 12, 1–87, 2012.

Li, C., Mao, J., Lau, A. K., Yuan, Z., Wang, M., & Liu, X. (2005). Application of MODIS satellite products to the air pollution research in Beijing. Science in China Series D(Earth Sciences), 48, 209-219.

Livingston, J., Redemann, J., Shinozuka, Y., Johnson, R., Russell, P., Zhang, Q., Mattoo, S., Remer, L., Levy, R., Munchak, L., et al.: Comparison of MODIS 3 km and 10 km resolution aerosol optical depth retrievals over land with airborne sun photometer measurements during ARCTAS summer 2008, Atmospheric Chemistry and Physics, 14, 2015–2038, 2014.

Lyapustin, A., Wang, Y., and Frey, R.: An automatic cloud mask algorithm based on time series of MODIS measurements, Journal of Geophysical Research: Atmospheres, 113, D16207, doi: 10.1029/2007JD009641, 2008.

Lyapustin, A., Martonchik, J., Wang, Y., Laszlo, I., and Korkin, S.: Multiangle implementation of atmospheric correction (MAIAC): 1. Radiative transfer basis and look-up tables, Journal of Geophysical Research: Atmospheres, 116, D03210, doi: doi:10.1029/2010JD014985, 2011a.

Lyapustin, A., Wang, Y., Hsu, C., Torres, O., Leptoukh, G., Kalashnikova, O., and Korkin, S.: Analysis of MAIAC dust aerosol retrievals from MODIS over North Africa, AAPP — Physical, Mathematical, and Natural Sciences, 89, ELS XIII Conference, Vol.89, Supplement No 1, 2011b.

Lyapustin, A., Wang, Y., Laszlo, I., Kahn, R., Korkin, S., Remer, L., Levy, R., and Reid, J. S.: Multiangle implementation of atmospheric correction (MAIAC): 2. Aerosol algorithm, Journal of Geophysical Research: Atmospheres, 116, D03211, doi: 10.1029/2010JD014986, 2011c.

Lyapustin, A. I., Wang, Y., Laszlo, I., Hilker, T., G.Hall, F., Sellers, P. J., Tucker, C. J., and Korkin, S. V.: Multi-angle implementation of atmospheric correction for MODIS (MAIAC): 3. Atmospheric correction, Remote Sensing of Environment, 127, 385 – 393, 2012.

Mazzola, M., Lanconelli, C., Lupi, A., Busetto, M., Vitale, V., and Tomasi, C.: Columnar aerosol optical properties in the Po Valley, Italy, from MFRSR data, Journal of Geophysical Research: Atmospheres, 115, D17206, doi: 10.1029/2009JD013310, 2010.

Mélin, F., and G. Zibordi (2005), Aerosol variability in the Po Valley analyzed from automated optical measurements, Geophys. Res. Lett., 32, L03810, doi:10.1029/2004GL021787.

Munchak, L., Levy, R., Mattoo, S., Remer, L., Holben, B., Schafer, J., Hostetler, C., and Ferrare, R.: MODIS 3 km aerosol product: applications over land in an urban/suburban region, Atmos. Meas. Tech., 6, 1747-1759, doi: 10.5194/amt-6-1747-2013, 2013.

Pope, C. A., Burnett, R. T., Thurston, G. D., Thun, M. J., Calle, E. E., Krewski, D., and Godleski, J. J.: Cardiovascular Mortality and Long-Term Exposure to Particulate Air Pollution: Epidemiological Evidence of General Patho- physiological Pathways of Disease, Circulation, 109, 71–77, 2004.

Putaud, J.-P., Raes, F., Dingenen, R. V., Bru¨ggemann, E., Facchini, M.-C., Decesari, S., Fuzzi, S., Gehrig, R., Hu¨glin, C., Laj, P., Lorbeer, G., Maenhaut, W., Mihalopoulos, N., Mu¨ller, K., Querol, X., Rodriguez, S., Schneider, J., Spindler, G., ten Brink, H., Tørseth, K., and Wiedensohler, A.: A European aerosol phenomenology—2: chemical characteristics of particulate matter at kerbside, urban, rural and background sites in Europe, Atmospheric Environment, 38, 2579 – 2595, 2004.

Putaud , J.-P., Dingenen, R. V., Alastuey, A., Bauer, H., Birmili, W., Cyrys, J., Flentje, H., Fuzzi, S., Gehrig, R., Hansson, H., Harrison, R., Herrmann, H., Hitzenberger, R., Hu¨glin, C., Jones, A., Kasper-Giebl, A., Kiss, G., Kousa, A., Kuhlbusch, T., Lo¨schau, G., Maenhaut, W.,

Molnar, A., Moreno, T., Pekkanen, J., Perrino, C., Pitz, M., Puxbaum, H., Querol, X., Rodriguez, S., Salma, I., Schwarz, J., Smolik, J., Schneider, J., Spindler, G., ten Brink, H., Tursic, J., Viana, M., Wiedensohler, A., and Raes, F.: A European aerosol phenomenology – 3: Physical and chemical characteristics of particulate matter from 60 rural, urban, and kerbside sites across Europe, Atmospheric Environment, 44, 1308 – 1320, 2010.

Putaud, J. P., Cavalli, F., Martins dos Santos, S., & Dell'Acqua, A. (2014). Long-term trends in aerosol optical characteristics in the Po Valley, Italy. *Atmospheric Chemistry and Physics*, *14*(17), 9129-9136.

Randriamiarisoa, H., Chazette, P., Couvert, P., Sanak, J., & Mégie, G. (2006). Relative humidity impact on aerosol parameters in a Paris suburban area. Atmospheric Chemistry and Physics, 6(5), 1389-1407.

Remer, L. A., Kaufman, Y. J., Tanré, D., Mattoo, S., Chu, D. A., Martins, J. V., Li, R.-R., Ichoku, C., Levy, R. C., Kleidman, R. G., Eck, T. F., Vermote, E., and Holben, B. N.: The MODIS Aerosol Algorithm, Products, and Validation, J. Atmos. Sci., 62, 947–973, 2005.

Remer, L. A., Tanre, D., Kaufman, Y. J., Levy, R., and Mattoo, S.: Algorithm for Remote Sensing of Tropospheric Aerosol from MODIS for Collection 005: Revision 2 National Aeronautics and Space Administration, Algorithm Theoretical Basis Document, available at http://modis- atmos.gsfc.nasa.gov/reference_atbd.html, 2009.

Remer, L. A., Mattoo, S., Levy, R. C., and Munchak, L. A.: MODIS 3 km aerosol product: algorithm and global perspective, Atmos. Meas. Tech., 6, 1829–1844, doi:10.5194/amt-6-1829- 2013, 2013.

Seidel, D. J., Zhang, Y., Beljaars, A., Golaz, J. C., Jacobson, A. R., & Medeiros, B. (2012). Climatology of the planetary boundary layer over the continental United States and Europe. Journal of Geophysical Research: Atmospheres (1984–2012), 117(D17).

Tian, J. and Chen, D.: A semi-empirical model for predicting hourly ground-level fine particulate matter (PM2.5) concentration in southern Ontario from satellite re- 865 mote sensing and ground-based meteorological measurements, Remote Sensing of Environment, 114, 221 – 229, 2010.

Troen, I. and L. Mahrt, 1986. "A Simple Model of the Atmospheric Boundary Layer: Sensitivity to Surface Evaporation." Boundary Layer Meteorology. Vol. 37, pp. 129-148.

Tsai, T.-C., Jeng, Y.-J., Chu, D. A., Chen, J.-P., and Chang, S.-C.: Analysis of the relationship between MODIS aerosol optical depth and particulate matter from 2006 to 2008, Atmospheric Environment, 45, 4777 – 4788, 2011.

van Donkelaar, A., Martin, R. V., and Park, R. J.: Estimating ground-level PM2.5 using aerosol optical depth determined from satellite remote sensing, Journal of Geophysical Research: Atmospheres, 111, D21201, doi: 10.1029/2005JD006996, 2006.

Wang, J. and Christopher, S.A.: Intercomparison between satellite derived aerosol optical thickness and PM2.5 mass: Implications for air quality studies, Geophysical Research Letters, 30, NO. 21, 2095, doi: 10.1029/2003GL018174, 2003.

Wang, J., & Martin, S. T. (2007). Satellite characterization of urban aerosols: Importance of including hygroscopicity and mixing state in the retrieval algorithms. Journal of Geophysical Research: Atmospheres (1984–2012), 112(D17).

Winker, D. M., Pelon J. and McCormick__, M. P., "The CALIPSO mission: spaceborne lidar for observation of aerosols and clouds", *Proc. SPIE* 4893, Lidar Remote Sensing for Industry and Environment Monitoring III, 1 (March 24, 2003); doi:10.1117/12.466539

Winker, D. M., Vaughan, M. A., Omar, A., Hu, Y., Powell, K. A., Liu, Z., Hunt, W. H., and Young, S. A.: Overview of the CALIPSO Mission and CALIOP Data Processing Algorithms, J. Atmos. Oceanic Technol., 26, 2310–2323, 2009.

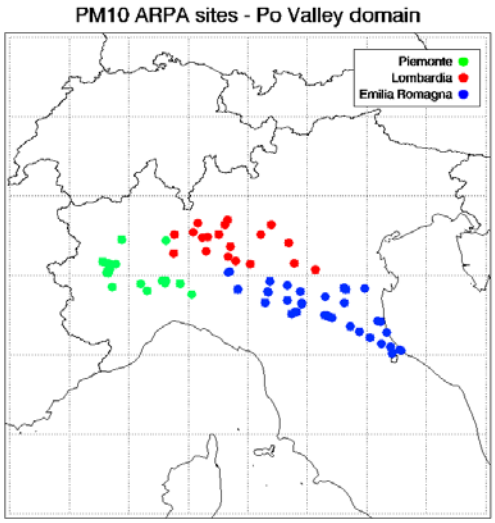

Figure 1. In the figure, the geographic study domain. The colored dots mark locations of the ARPA PM_{10} ground-based stations; they are grouped into different color to respect the administrative division of the sites (Piemonte in green, Lombardia in red and Emilia Romagna in blue).

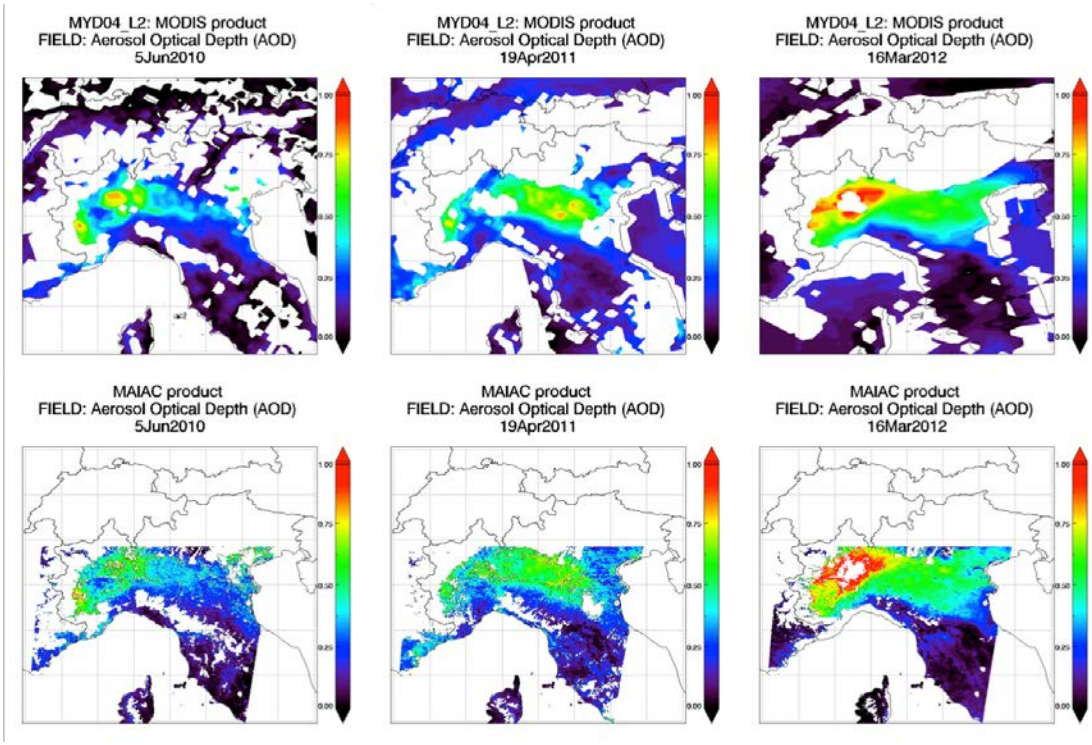

Figure 2. MYD04 10 km (on the top) and MAIAC 1 km (on the bottom) AOD retrievals for three example days, one per each year of analysis (2010, 2011 and 2012). The higher resolution data reveals a substantial spatial variability of AOD, which is not as well captured using a coarse 10 km scale, especially near the urban areas, and near the sea cost.

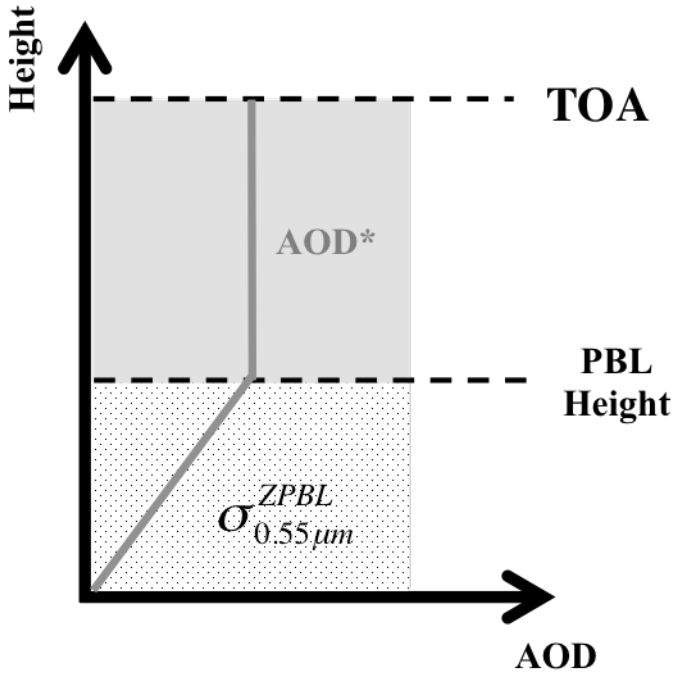

Figure 3. Schematic aerosol vertical profile where the aerosols are considered well-mixed and confined in the PBL height.

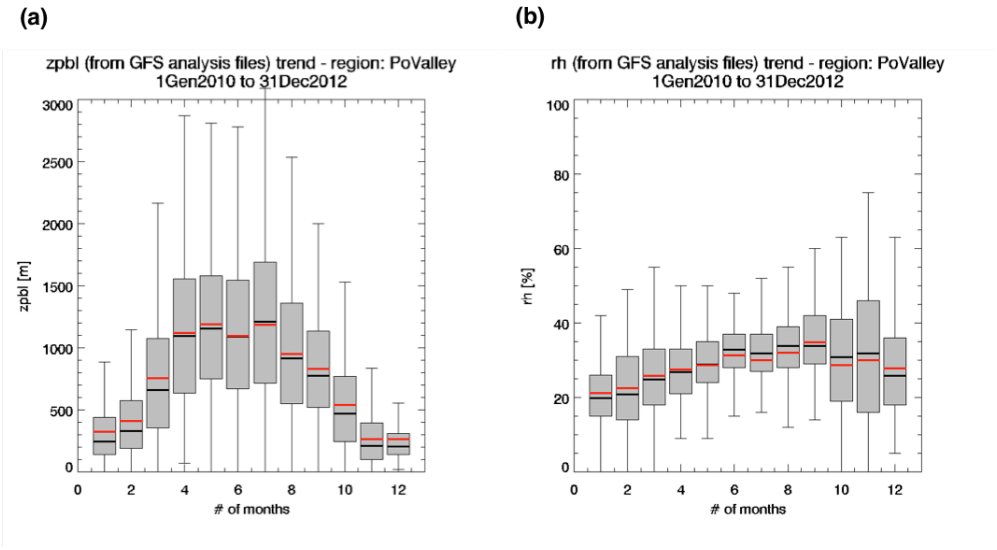

Figure 4. PBL depth and RH monthly trends, from 2010 and 2012. For each candlestick, the 10^{th}, 25^{th}, 50^{th} (median, horizontal black thick line), 75^{th}, 90^{th} are shown as horizontal black bars. The red thick line represents the monthly mean value. The graph was realized considering all the equals months in the period of analysis.

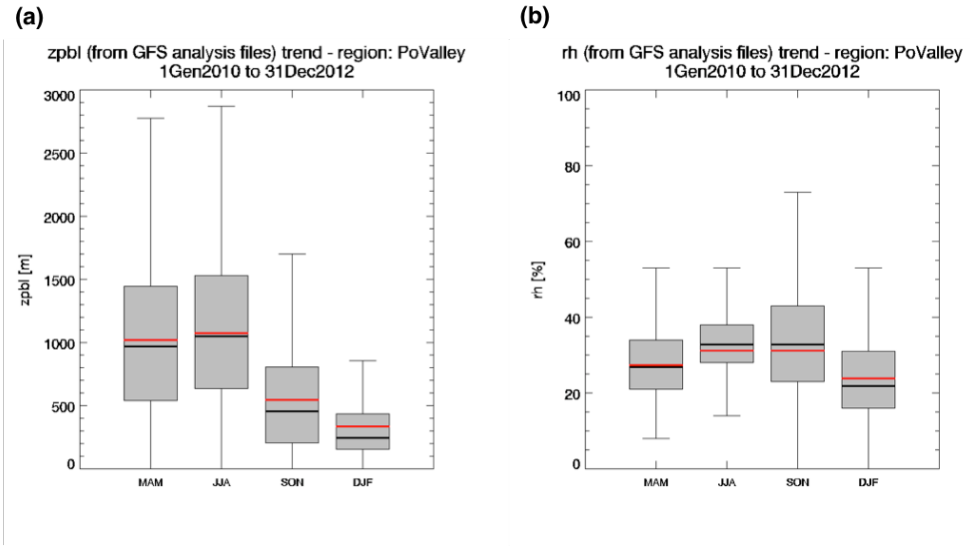

Figure 5. PBL depth and RH seasonal trends, from 2010 and 2012. MAM (March, April, May) refers to the spring months; JJA (June, July, August) refers to the summer months; SON (September, October, November) refers to the fall month and DJF (December, January, February) refers to the winter months. For each candlestick, the 10^{th}, 25^{th}, 50^{th} (median, horizontal black thick line), 75^{th}, 90^{th} are shown as horizontal black bars. The red thick line represents the seasonal mean value. The graph was realized considering all the equal months in the period of analysis (3 years) and then grouped into the four seasons.

Table 1. Global statistics values for the direct PM_{10} – MYD04 and PM_{10} – MAIAC AOD linear correlations, with and without ZPBL normalization and RH correction, for the period from 2010 to 2012, for the same days and locations.

		Correlation type	Statistics			
			Intercept	**Slope**	**R^2**	***p*-value**
MYD04	**2010-2012**	PM_{10}; AOD	21.35	30.23	0.09	<0.0001
		PM_{10}; AOD_{ZPBL}	22.59	17.94	0.21	<0.0001
		PM_{10}*f(RH); AOD_{ZPBL}	31.63	23.98	0.22	<0.0001
MAIAC	**2010-2012**	PM_{10}; AOD	28.49	20.81	0.02	<0.0001
		PM_{10}; AOD_{ZPBL}	23.64	21.71	0.29	<0.0001
		PM_{10}*f(RH); AOD_{ZPBL}	31.96	27.53	0.29	<0.0001

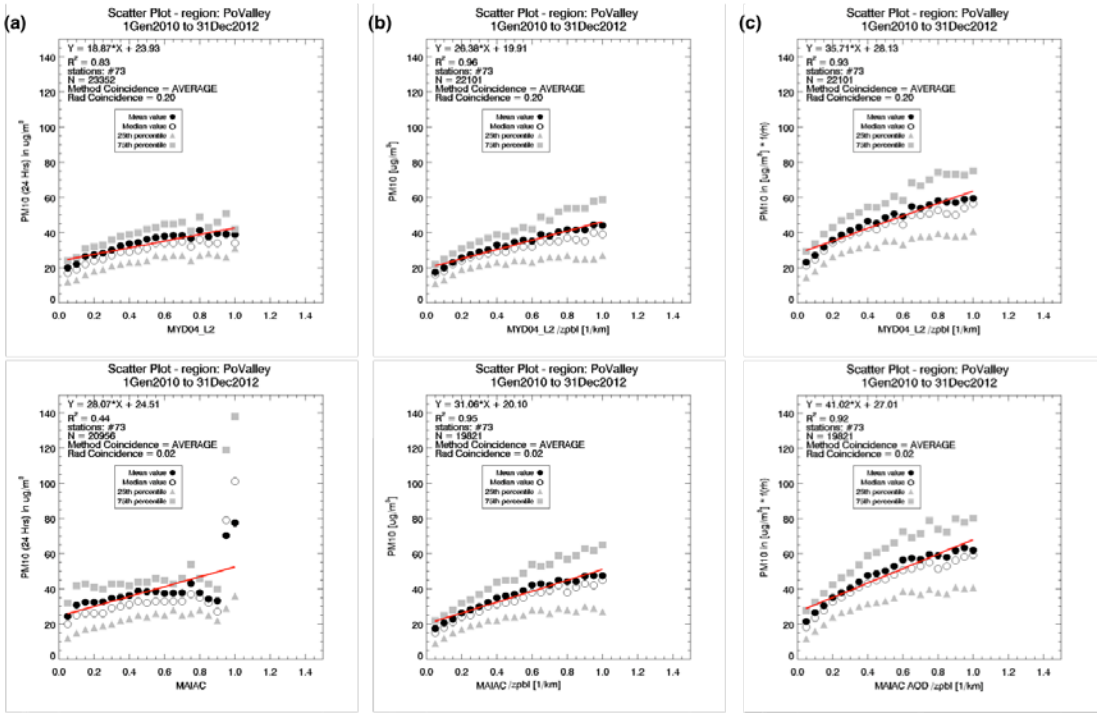

Figure 6. Correlation between PM_{10} and MYD04_L2 and MAIAC AOD at Po Valley ground-based stations from 2010 to 2012. Bin scatter plot analysis presented for both retrievals (MYD04_L2 top panels, MAIAC bottom panels). Panels (a): simple correlation between PM_{10} and AOD; panels (b) correlation between PM_{10} and AOD normalized by ZPBL; panels (c) correlation between PM_{10} corrected by RH and AOD normalized by ZPBL.

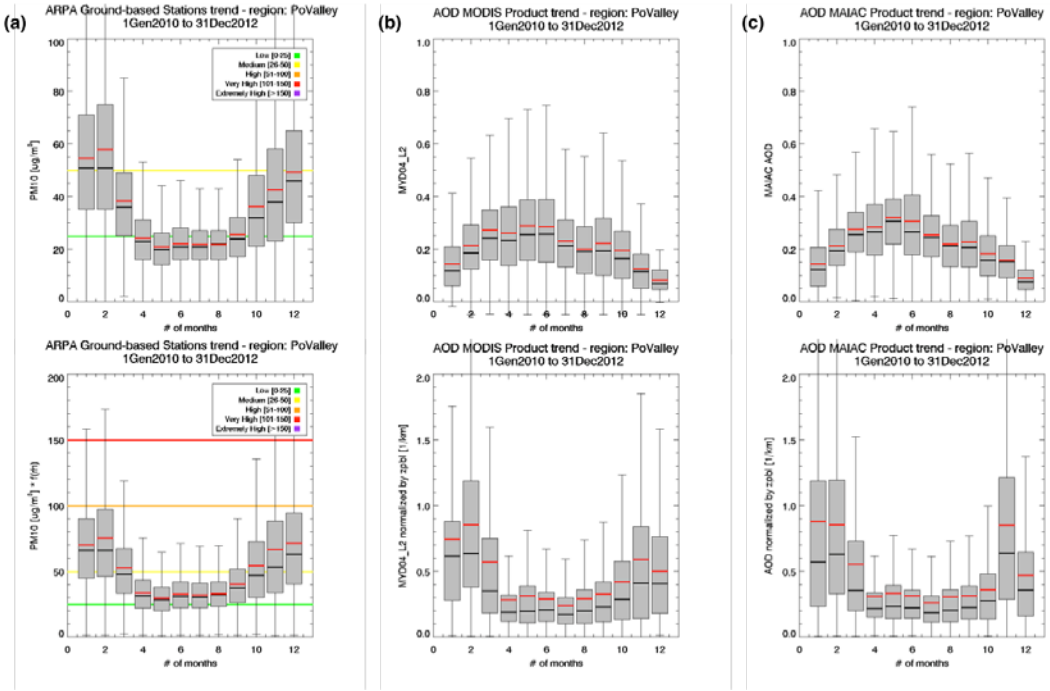

Figure 7. PM_{10} and AOD (both for MYD04_L2 and MAIAC retrievals) monthly trends, from 2010 and 2012. In panels (a), the PM_{10} monthly trend (top) is compared to the PM_{10} trend multiple by the RH correction (bottom). In panels (b) and (c) the AOD monthly trends, for MODIS and MAIAC AOD respectively, are compared with the AOD trend normalized by the PBL depth value. For each candlestick, the 10^{th}, 25^{th}, 50^{th} (median, horizontal black thick line), 75^{th}, 90^{th} are shown as horizontal black bars. The red thick line represents the monthly mean value. The graph was realized considering all the equals months in the period of analysis.

Table 2. PM_{10} and AOD total available data

Total presumed data (tpd)	**N_{tot} = 73 (#stations) * 1096(days) = 80008**
total PM_{10} retrieved data (trd_PM_{10})	N_{PM10} = 74357
(trd_PM_{10})/(tpd)	93%
total MYD04 retrieved data (trd_AOD)	N_{MYD04} = 25697
(trd_MYD04)/(tpd)	32%
total MAIAC retrieved data (trd_AOD)	N_{MAIAC} = 22547
(trd_MAIAC)/(tpd)	28%

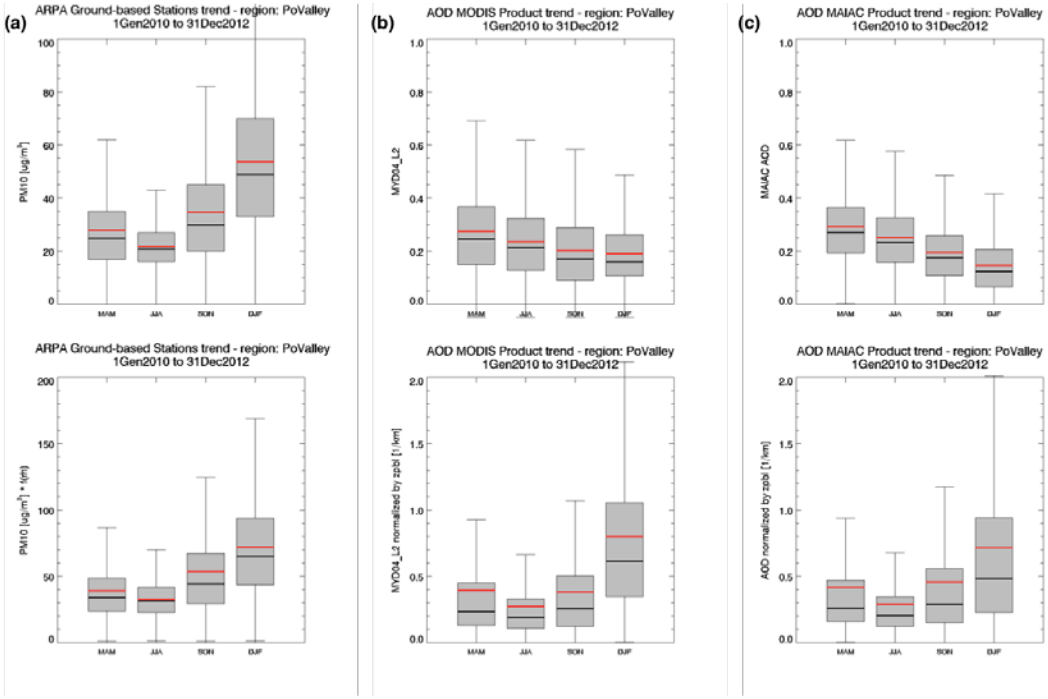

Figure 8. PM_{10} and AOD (both for MYD04_L2 and MAIAC retrievals) seasonal trends, from 2010 and 2012. In panels (a), the PM_{10} seasonal trend (top) is compared to the PM_{10} trend multiple by the RH correction (bottom). In panels (b) and (c) the AOD monthly trends, for MODIS and MAIAC AOD respectively, are compared with the AOD trend normalized by the PBL depth value. MAM (March, April, May) refers to the spring months; JJA (June, July, August) refers to the summer months; SON (September, October, November) refers to the fall month and DJF (December, January, February) refers to the winter months. For each candlestick, the 10^{th}, 25^{th}, 50^{th} (median, horizontal black thick line), 75^{th}, 90^{th} are shown as horizontal black bars. The red thick line represents the monthly mean value. The graph was realized considering all the equal months in the period of analysis (3 years) and then grouped into the four seasons.

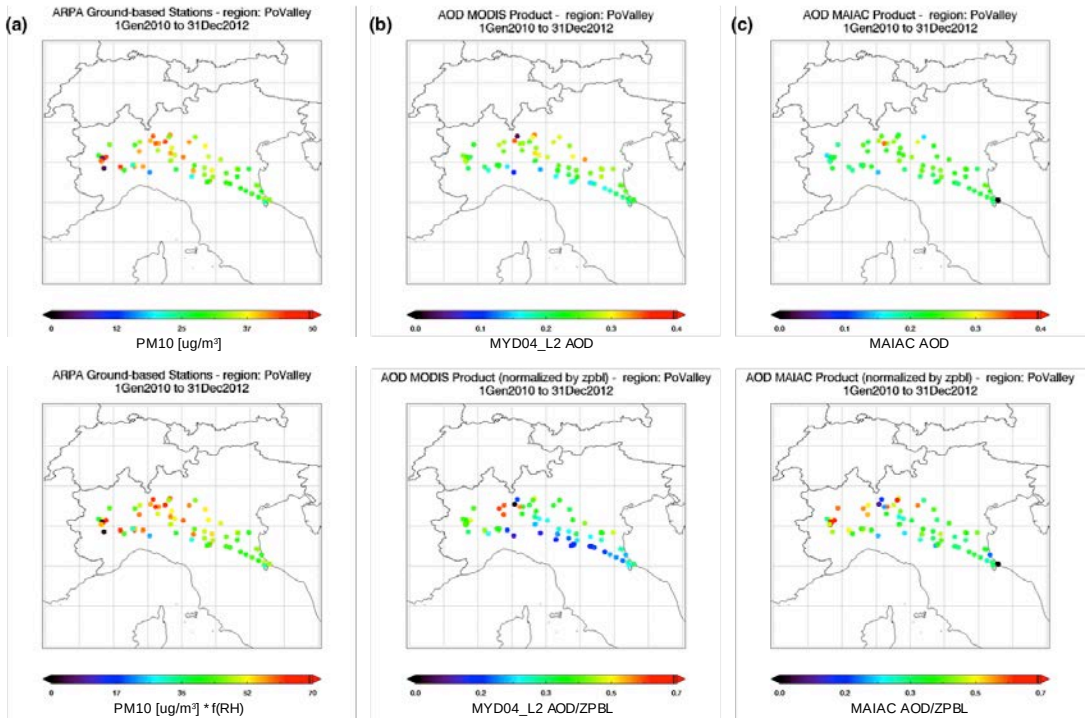

Figure 9. Panels (a): annual mean PM_{10} concentration measured from ARPA ground-based stations, without (top) and with (bottom) the RH correction. Panels (b) and (c): annual mean MODIS and MAIAC AOD retrievals, respectively, without (top) and with (bottom) the normalization from the PBL depth. All the results refer to the entire period and locations of analysis.

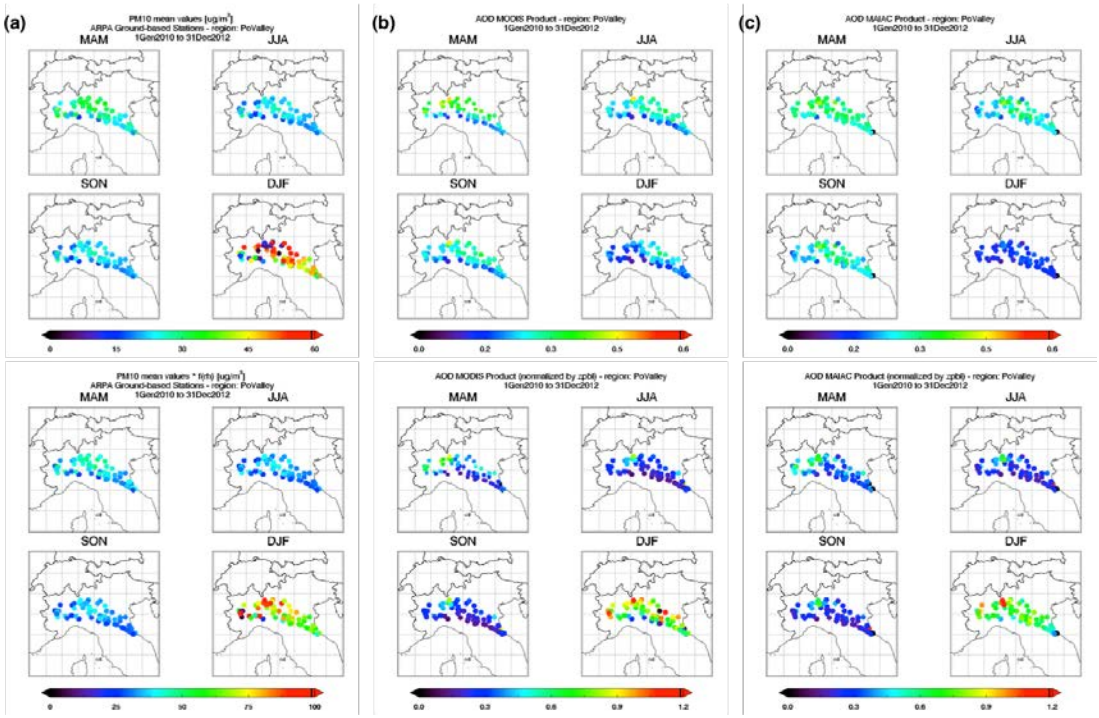

Figure 10. Panels (a): seasonal mean PM_{10} concentration measured from ARPA ground-based stations, without (top) and with (bottom) the RH correction. Panels (b) and (c): seasonal mean MODIS and MAIAC AOD retrievals, respectively, without (top) and with (bottom) the normalization from the PBL depth. In each panels, the mean values are grouped into the four seasons: MAM (March, April, May) refers to the spring months; JJA (June, July, August) refers to the summer months; SON (September, October, November) refers to the fall month and DJF (December, January, February) refers to the winter months.

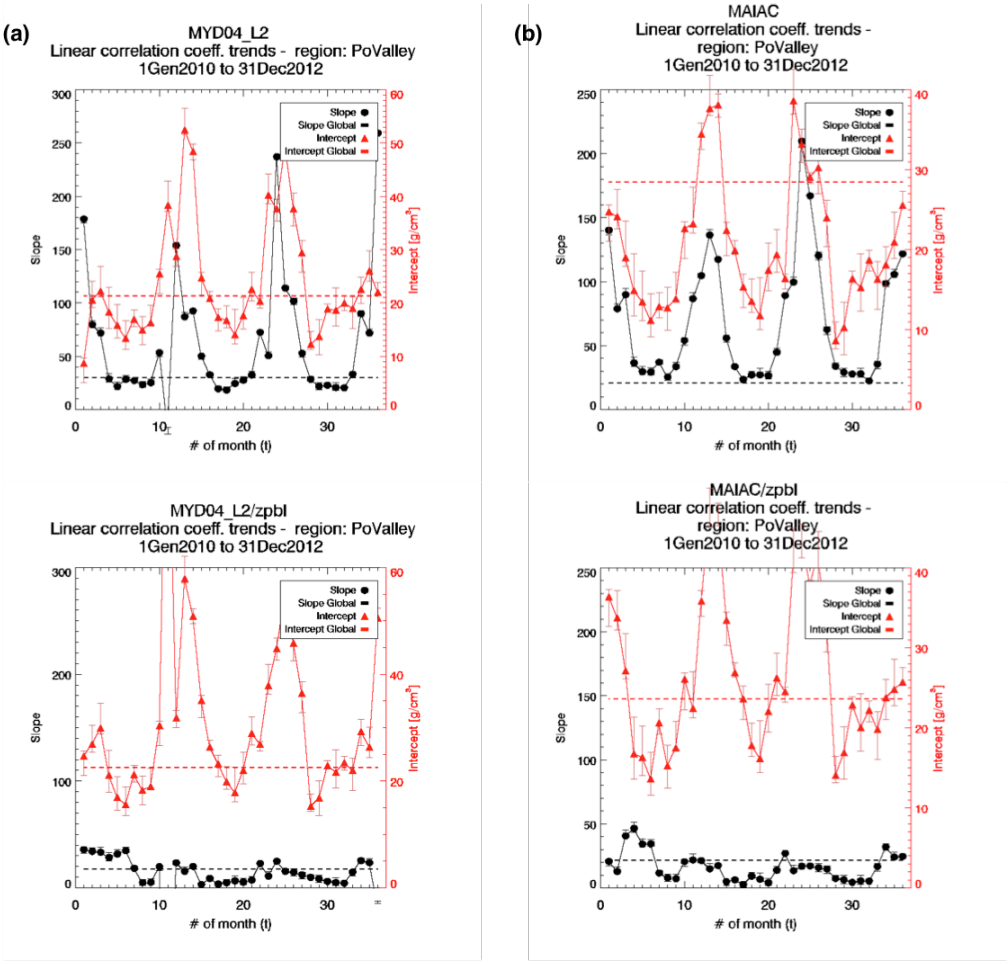

Figure 11. Linear correlation coefficients monthly trends for the MYD04_L2 and MAIAC AOD dataset. Coefficient "slope" of the linear correlation in black; in red, the "intercept" coefficient, both for the period from 2010 to 2012. The dash lines on the graph refer to the intercept and slope values obtained from the entire dataset, for the entire period.

1 Table 3. Seasonal statistics coefficients obtained from the linear correlation PM_{10} –
2 MYD04/MAIAC AOD datasets, with and without the ZPBL normalization, considering the
3 total period of analysis from 2010 to 2012, and locations.

	Correlation type	Statistics					
		Intercept (q)		Slope (m)		R^2	
		MYD04_L2	MAIAC	MYD04_L2	MAIAC	MYD04_L2	MAIAC
MAM	PM_{10}; AOD	19.46	16.46	36.53	43.94	0.20	0.19
	PM_{10}; AOD_{ZPBL}	24.63	23.18	15.63	18.36	0.13	0.12
JJA	PM_{10}; AOD	16.85	14.47	23.82	27.93	0.19	0.21
	PM_{10}; AOD_{ZPBL}	20.37	19.00	10.21	10.06	0.08	0.09
SON	PM_{10}; AOD	25.70	21.10	45.43	72.08	0.19	0.20
	PM_{10}; AOD_{ZPBL}	36.28	25.17	-8.04	19.79	0.21	0.19
DJF	PM_{10}; AOD	34.03	30.83	145.08	133.08	0.31	0.18
	PM_{10}; AOD_{ZPBL}	43.25	38.64	19.02	18.16	0.27	0.19

4

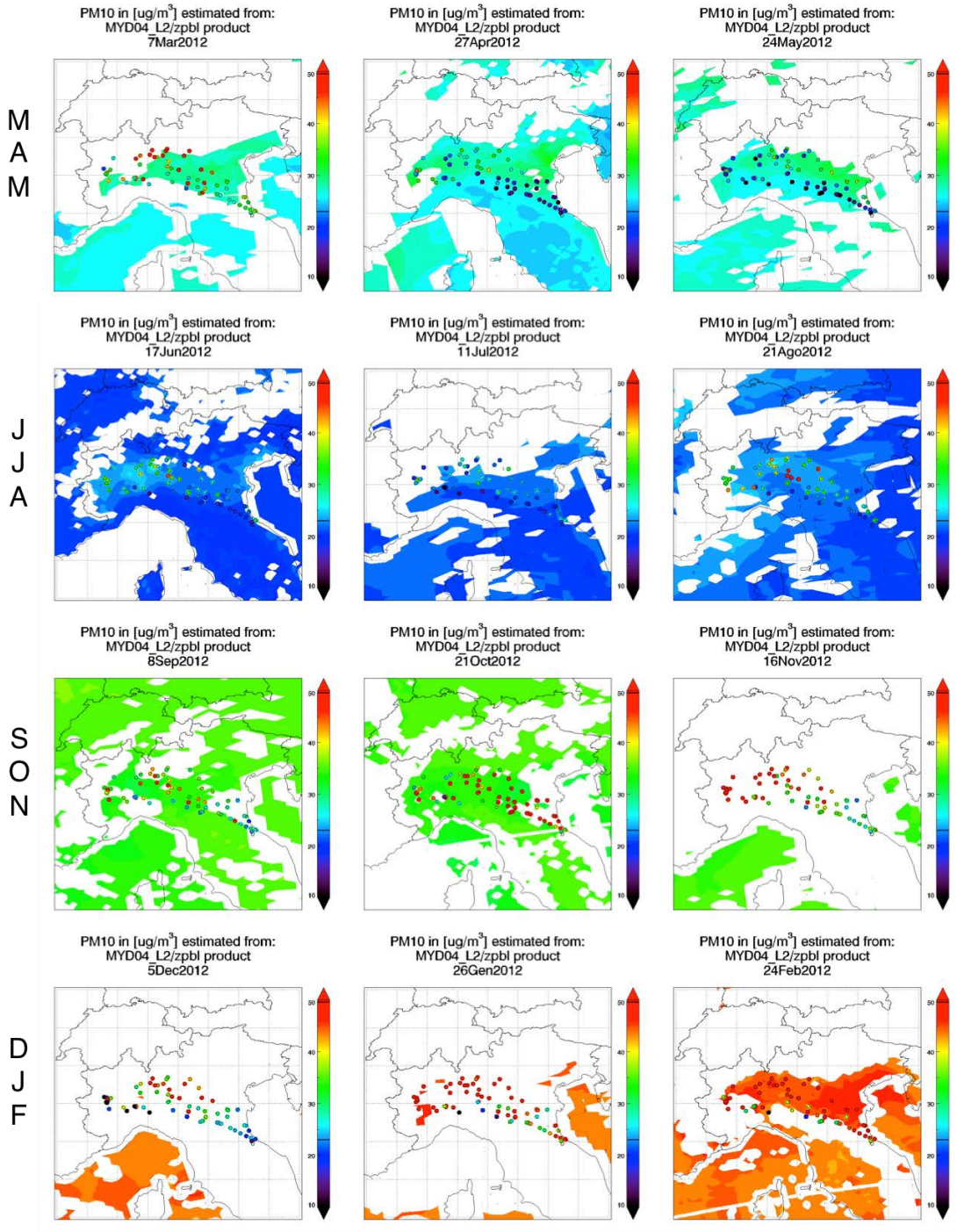

Figure 12. Estimated pollutant PM_{10} values from the MYD04 AOD retrieval normalized by the PBL depth. On the basemap the PM_{10} ground-based sites measurements are overlapped. An example day per each month of the year (2012) is reported, dived into the four seasons.

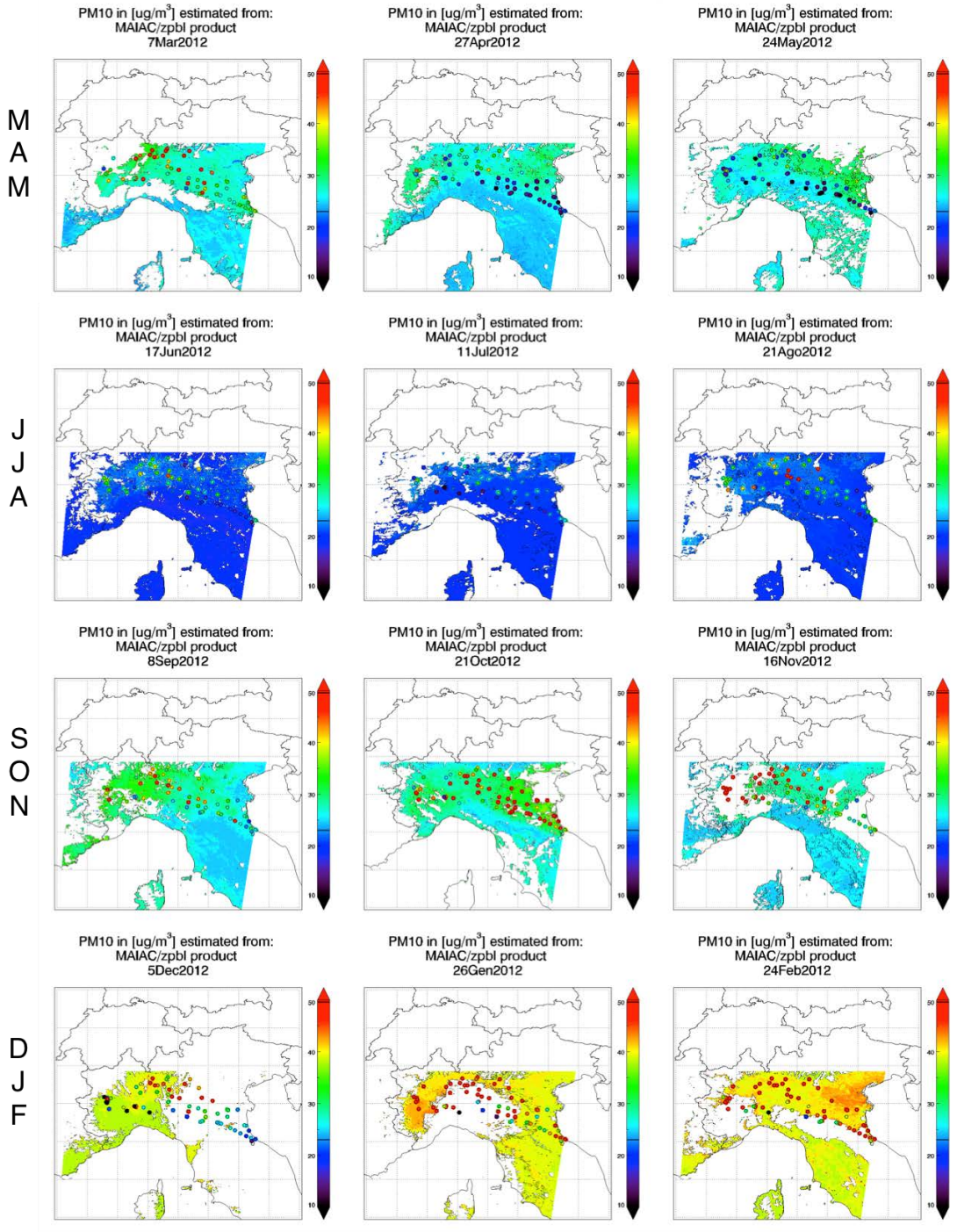

Figure 13. Estimated pollutant PM_{10} values from the high-resolution MAIAC AOD retrieval normalized by the PBL depth. On the basemap the PM_{10} ground-based sites measurements are overlapped. An example day per each month of the year (2012) is reported, divided into the four seasons.

Table 4. RMSE seasonal values obtained between the measured and estimated PM_{10} concentrations. The pollutant was estimated by both MYD04_L2 and MAIAC AOD dataset, with and without the ZPBL normalization, considering the total period of analysis from 2010 to 2012.

		RMSE [µg/m³]		**R^2**	
	Correlation type	**MYD04_L2**	**MAIAC**	**MYD04_L2**	**MAIAC**
MAM	PM_{10}; AOD	8.58	8.06	0.29	0.23
	PM_{10}; AOD_{ZPBL}	8.33	7.89	0.31	0.18
JJA	PM_{10}; AOD	6.91	6.63	0.46	0.26
	PM_{10}; AOD_{ZPBL}	6.78	6.45	0.46	0.20
SON	PM_{10}; AOD	7.82	9.03	0.17	0.22
	PM_{10}; AOD_{ZPBL}	6.44	7.22	0.18	0.16
DJF	PM_{10}; AOD	7.54	15.10	0.04	0.16
	PM_{10}; AOD_{ZPBL}	5.33	11.45	0.04	0.13